
Is a Pure Transformer Effective for Separated and Online Multi-Object Tracking?

Chongwei Liu¹ Haojie Li^{1,2} Zhihui Wang¹ Rui Xu^{1*}

¹Dalian University of Technology

²Shandong University of Science and Technology

lcwdllg@mail.dlut.edu.cn hjli@sdust.edu.cn

zhwang@dlut.edu.cn xurui@dlut.edu.cn

Abstract

Recent advances in Multi-Object Tracking (MOT) have demonstrated significant success in short-term association within the separated tracking-by-detection online paradigm. However, long-term tracking remains challenging. While graph-based approaches address this by modeling trajectories as global graphs, these methods are unsuitable for real-time applications due to their non-online nature. In this paper, we review the concept of trajectory graphs and propose a novel perspective by representing them as directed acyclic graphs. This representation can be described using frame-ordered object sequences and binary adjacency matrices. We observe that this structure naturally aligns with Transformer attention mechanisms, enabling us to model the association problem using a classic Transformer architecture. Based on this insight, we introduce a concise Pure Transformer (PuTR) to validate the effectiveness of Transformer in unifying short- and long-term tracking for separated online MOT. Extensive experiments on four diverse datasets (SportsMOT, DanceTrack, MOT17, and MOT20) demonstrate that PuTR effectively establishes a solid baseline compared to existing foundational online methods while exhibiting superior domain adaptation capabilities. Furthermore, the separated nature enables efficient training and inference, making it suitable for practical applications. Implementation code and trained models are available at <https://github.com/chongweiliu/PuTR>.

1 Introduction

Multi-Object Tracking (MOT) is a fundamental computer vision task essential for modern perception systems, ranging from autonomous driving [14] to video surveillance [13] and behavior analysis [20]. The field has witnessed diverse methodological approaches, including motion estimation [4; 60] and graph-based techniques [22; 5].

Among these methodologies, the separated tracking-by-detection (TbD) online paradigm has become dominant due to its effectiveness and simplicity. This approach separates MOT into two distinct tasks: object detection and cross-frame association. Using ready-made detectors like YOLOX [17], it treats frame-by-frame detection results as immutable and focuses on solving the association problem. Methods such as SORT [4] and ByteTrack [60] demonstrate this approach’s effectiveness, using Kalman filtering [23] for motion prediction and the Hungarian algorithm [24] for Intersection-over-Union (IoU) based association. While these handcrafted heuristic approaches excel in short-term tracking scenarios without data-driven learning, they inherently struggle with long-term tracking when relying solely on motion information.

The long-term tracking — maintaining object identity through extended occlusions or absences — remains a significant challenge for above heuristic approaches. These methods lack a unified

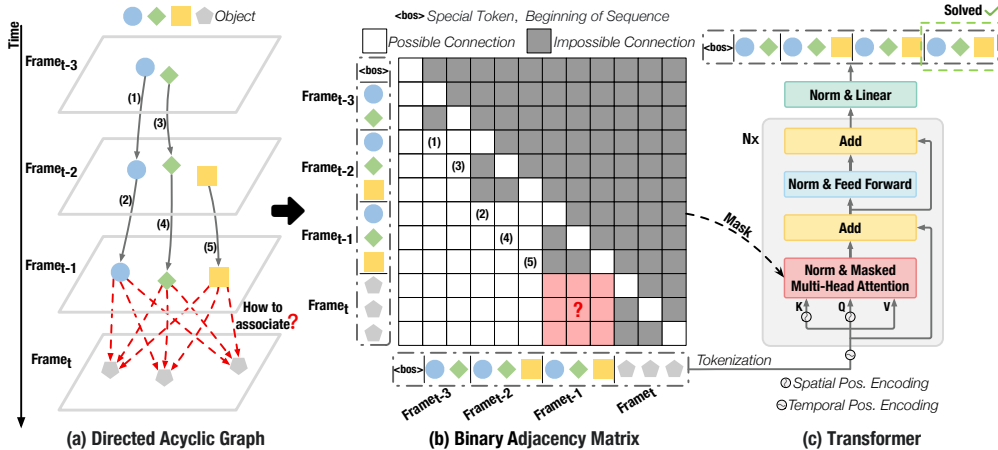


Figure 1: Illustration of our chain of thought. Trajectories are inherently a directed acyclic graph in the temporal order (a). We can thus transform it equivalently into a binary adjacency matrix (b), exactly aligning with the Transformer’s attention mask. Consequently, arranging objects by frame forms a natural input sequence for the Transformer (c), enabling it to model the association problem.

framework for modeling both short- and long-term associations, often resorting to complex hand-crafted rules or additional components [7; 52] for long-term tracking. In response, graph-based methods [5; 9] have emerged, modeling trajectories as global graphs and employing Graph Neural Networks (GNNs) [38] for association. While these approaches effectively handle both short- and long-term scenarios through global context modeling, they sacrifice online processing capability, limiting their real-time applicability.

This leads us to a fundamental question: How can we elegantly unify short- and long-term tracking challenges while maintaining a separated and online manner? Our key insight, illustrated in Fig.1, stems from recognizing that trajectory graphs are inherently directed acyclic graphs (DAGs), i.e., each trajectory propagates independently in time, with nodes constrained to at most one in-degree and one out-degree. This structure enables representation as a frame-ordered object sequence with a binary adjacency matrix (Fig.1b). Notably, this matrix’s structure — comprising white blocks for possible connections and gray blocks for impossible ones — mirrors the attention mask in Transformer architectures [45] (Fig.1c). This structural alignment motivates our intuition: trajectory graphs can be naturally modeled via a pure Transformer in an online and separated paradigm, complementing traditional non-online graph-based methods.

Previous works like TrackFormer [30] and MOTR [58] have already incorporated Transformers into MOT by adapting the Transformer-based detector DETR [8] for end-to-end tracking. The key difference between these works and our idea is the track propagation mechanism. They modify Deformable-DETR [64] to propagate tracklets across frames via query tokens to perform detection and association simultaneously. This propagation trait stems from earlier works like Tracktor [2] and CenterTrack [62], which utilized CNN-based detectors [34; 63] at that time. However, their track propagation mechanism more closely resembles RNN [37] behavior rather than a true Transformer, and the Transformer structure is only used for detection. *In these cases, the true power of the self-attention mechanism to model context dependencies is not exploited for association tasks. Our straightforward idea is to leverage the potential of Transformers for the association problem, thereby opening up a new and promising research direction in the field of MOT.*

In this paper, we present **Pure Transformer (PuTR)**, a concise architecture that validates our intuitive idea. Following Occam’s Razor, we utilize established practices for adapting the Transformer to MOT. As Fig.1c shows, we modify the attention mask and incorporate temporal and spatial positional encodings to adapt it to the unique characteristics of the object sequence compared to a normal text sequence. Specifically, unlike a sentence, the object sequence is ordered in the outer frame temporal dimension but unordered in the inner image spatial dimension. Therefore, we modify the attention mask to ensure permutation invariance within the same frame and introduce temporal and spatial positional encodings to encode the frame order and the object coordinate information into the object sequence. We conduct experiments on four MOT datasets: SportsMOT [10], DanceTrack [41], MOT17 [31], and MOT20 [11], to demonstrate the effectiveness of our approach. The results show

that PuTR achieves a solid baseline compared to existing foundational online methods. Notably, PuTR exhibits superior domain adaptation ability, with a maximum cross-dataset gap of only 1.7% in HOTA without fine-tuning. Furthermore, PuTR is efficient in both training and inference. It can be trained from scratch on a single GPU in one hour without additional data or complex training processes, and achieves up to 77 FPS in inference when given detection results.

In summary, our main contributions are:

- We review the trajectory graph and discover that it naturally aligns with the Transformer architecture, providing a theoretical foundation for applying Transformers to solve the association problem in multi-object tracking.
- We propose a concise Pure Transformer architecture (PuTR) to validate our intuitive idea. By inputting the object sequence in temporal order, our approach maintains online processing capability while naturally unifying short- and long-term object associations.
- We conduct experiments on four datasets to demonstrate the effectiveness of our approach in terms of performance, domain adaptation, and efficiency. The results show that PuTR achieves a solid baseline compared to existing foundational online methods.

2 Related Work

The MOT field has witnessed diverse approaches to address the challenging association problem. We provide a concise overview of the most representative methodologies.

2.1 Heuristic Methods

Heuristic methods constitute the dominant paradigm in MOT. Following the separated paradigm, these approaches first employ pre-trained detectors [34; 17; 63] for frame-wise object detection, followed by online cross-frame association. Given the fixed nature of detection results, research efforts primarily concentrate on the association problem, with particular emphasis on motion modeling and spatial relationships.

SORT [4] established the foundational framework by integrating Kalman filtering[23] for motion prediction with the Hungarian algorithm[24] for association, while introducing a runtime manager system for tracklets (*Track*, *Lost*, and *New*). Subsequent research has largely built upon SORT’s architecture, enhancing association robustness through various strategies: integrating appearance features via dedicated ReID models [48; 12; 52; 56], developing advanced motion models [60; 7; 21], and incorporating camera motion compensation [1; 29; 54].

Despite their effectiveness in short-term tracking scenarios, these approaches face inherent limitations in unifying short-term and long-term tracking within a single theoretical framework. Maintaining tracklet completeness in long-term scenarios often requires additional complex handcrafted rules, highlighting the fundamental constraints of this methodology.

2.2 Graph-based Methods

Graph-based approaches have emerged as a promising alternative to address the inherent limitations of heuristic methods. Within the separated paradigm, these approaches formulate MOT as a graph optimization problem, where detected objects serve as nodes and trajectory hypotheses as edges. Unlike traditional frame-by-frame trackers, graph-based methods pursue global solutions for data association across multiple frames or entire sequences, achieving robust performance in semi-online or offline settings.

Early research in this domain explored various optimization frameworks, including fixed cost minimization [22; 33], multi-cuts [43], and minimum cliques [36]. Recent advances in GNNs have introduced more sophisticated approaches [5; 9]. MPNTrack [5] leverages message passing networks for detection association through edge classification, while SUSHI [9] implements recursive hierarchical levels to optimize graph space overhead and process extended video sequences. While these methods successfully unify short- and long-term tracking under a global perspective, their offline nature presents limitations for real-time applications.

Our key contribution stems from recognizing the inherent structure of trajectory graphs as DAGs. This insight enables a novel approach to modeling association problems using Transformers in a separated and online manner, effectively balancing comprehensive context modeling with real-time processing capabilities.

2.3 Detector-based Methods

Given that object detection is prerequisite for the TbD paradigm, efforts have emerged to integrate detection and tracking into unified, simultaneously trainable frameworks. Joint-Detection-and-Embedding (JDE) [47] and FairMOT [61] represent transitional approaches, modifying CNN-based detectors to generate both object boxes and appearance features for heuristic association [18; 32].

In the CNN era, unified frameworks like Tracktor [2] and CenterTrack [62] modified detectors to predict current tracklets from previous results [46; 42]. The Transformer era, dominated by the DETR family [8; 64; 26], saw TrackFormer [30] and MOTR [58] extend Deformable-DETR’s [64] object queries to MOT. Recent advances focus on historical object embedding storage [6; 15] and resolving conflicts between new and tracked object queries [51; 57]. Despite architectural evolution from CNN to Transformer, the core mechanism remains RNN-style tracklet state propagation. PuTR explores an alternative approach, focusing on association rather than detection.

MOTIP [16] similarly recognizes Transformers’ association potential, formulating tracking as end-to-end in-context ID prediction. It employs a learnable ID dictionary and Transformer decoder post-Deformable-DETR for tracking ID prediction, using historical trajectories as K and V , and current detections as Q in attention mechanisms, where K , Q , and V denote the *Key*, *Query*, and *Value* matrices, respectively. While conceptually similar, PuTR and MOTIP differ significantly in implementation. PuTR’s separated, decoder-only architecture enables efficient single-GPU training without pre-training or complex stabilization. Conversely, MOTIP’s end-to-end approach requires multi-GPU training and empirical ID dictionary tuning, while PuTR chooses learning assignment matrices directly [50] for relative affinity association to avoid such constraints, achieving superior domain adaptation.

We acknowledge that these methodologies are complementary rather than competitive. The runtime manager appears in DETR-based methods, while our approach draws from GNN-based trajectory graphs. MOTIP bridges MOTR and PuTR, with each method occupying distinct niches. End-to-end frameworks excel with sufficient video-level data (e.g., DanceTrack), while our separated approach provides a baseline for scarce-data scenarios (e.g., MOT17). We advocate for methodological coexistence, offering comprehensive solutions to the MOT community.

3 Method

This section introduces the implementation of PuTR, which leverages the Transformer’s self-attention mechanism to model the association problem in separated and online MOT. Section 3.1 presents the fundamental concepts and problem formulation of MOT and introduces the input object sequence and tokenization process. Section 3.2 provides details of the PuTR architecture, including modifications on causal masking and positional encoding. Sections 3.3 and 3.4 describe the training and inference processes, respectively.

3.1 Preliminary

We first introduce the fundamental concepts in PuTR. Our approach follows the TbD paradigm. Given a video, we assume that object detections are computed for every frame, and our task is to perform data association by linking object detections into online trajectories.

3.1.1 Problem Formulation

We denote the set of objects in the t -th frame as $\mathcal{O}_t = \{o_{tid}^t\}$, where o_{tid}^t represents the detected object with the tracking identity tid . Each o_{tid}^t is represented by its bounding box (bbox), confidence score, and category label. The tid is assigned to each object belonging to the same trajectory, with $tid = -1$ indicating that the object does not belong to any trajectory. Within an \mathcal{O}_t set, each tid is unique, except for -1 . The goal of association is to obtain the set of trajectories \mathcal{T}^* that group

detections corresponding to the same identity. Each trajectory $\mathcal{T}_k \in \mathcal{T}^*$ is given by its set of detections $\mathcal{T}_k = \{o_k^t \mid t_{s,k} \leq t \leq t_{e,k}\}$, where $t_{s,k}$ and $t_{e,k}$ are the start and end frames of the trajectory \mathcal{T}_k , respectively.

3.1.2 Input Object Sequence

Following Transformer manner, the PuTR input is also a sequence, but consisting of detections in recent $T+1$ consecutive frames. We denote the input object sequence as $\mathcal{S} = (\langle \text{bos} \rangle, \mathcal{O}_{t-T}, \dots, \mathcal{O}_t)$. Similar to large language models, \mathcal{S} starts with a special token $\langle \text{bos} \rangle$ to indicate the beginning of the sequence, which is an all-zero token. The input sequence is then fed into PuTR after tokenization.

3.1.3 Tokenization

To feed into PuTR, we first convert each object o_{iid}^t into a token representation. We denote the token representation of o_{iid}^t as x_{iid}^t and the corresponding token set as $\mathcal{X}_t = \{x_{iid}^t\}$. It is feasible to map objects into high-dimensional vectors by employing an independent Re-ID model [12] or DETR object embeddings [58]. However, in this work, to maintain simplicity and efficiency, we adopt a straightforward approach by directly encoding the object image patches from the raw image into token representations. Specifically, for each object image patch $p_{iid}^t \in \mathbb{R}^{h \times w \times 3}$, generated by cropping the corresponding object detection bbox¹ from the t -th frame (raw image), we divide it into a 64×64 grid and sample the center point of each grid via bilinear interpolation. We then flatten these points to obtain a 1-d representation $r_{iid}^t \in \mathbb{R}^{1 \times (64 \cdot 64 \cdot 3)}$, and pass it through a linear layer to obtain the tokenized representation x_{iid}^t with the same dimension as the PuTR model dimension $d_{model} = 512$. The tokenized sequence thus becomes $\mathcal{S}_{in} = (\langle \text{bos} \rangle, \mathcal{X}_{t-T}, \dots, \mathcal{X}_t) \in \mathbb{R}^{n_S \times d_{model}}$, where n_S is the token number of the sequence.

3.2 Architecture

3.2.1 Overview

As shown in Fig.1c, PuTR follows the standard Transformer architecture, composed of a stack of $N = 6$ identical layers. Each layer has two sub-layers: a masked multi-head self-attention mechanism with 8 heads, and a feed-forward network. A residual connection is employed around each sub-layer. To improve training stability, we perform normalization before each sub-layer input following Llama2 [44]. The \mathcal{S}_{in} is fed into PuTR after adding temporal positional encodings, and spatial positional encodings are added before being linearly projected into K and V in each attention mechanism. After the N layers, the output object embeddings are linearly projected into high-dimensional representations, denoted as $\mathcal{S}_{out} = (\langle \text{bos} \rangle, \mathcal{Z}_{t-T}, \dots, \mathcal{Z}_t) \in \mathbb{R}^{n_S \times d_{model}}$, which is then used to calculate the relative affinity matrix between trajectories and current detections to solve the association problem.

3.2.2 Modifications

Unlike sentences, object sequences are ordered temporally across frames but unordered spatially within each frame. To account for this, we modify the attention mask and introduce temporal and spatial positional encodings.

Since objects in \mathcal{O}_t are unordered and cannot be interlinked, we modify the conventional causal mask (a lower triangular matrix) to ensure permutation invariance within the same frame. Specifically, based on the causal mask, we additionally set the positions to zero for tokens in the same frame, i.e., $mask_{ij} = 0$ if $t_i == t_j$ & $i \neq j$, where t_i and t_j are the frame indices of the i -th and j -th tokens, respectively. We refer to this as the frame causal mask, which precisely aligns with the distribution of the white blocks in Fig.1b, and thus is consistent with the trajectory graph structure.

For positional encoding, we employ two distinct approaches. Temporally, we utilize the absolute positional encoding from the original Transformer to encode the frame order. Spatially, we adopt the method from DAB-DETR [26] to encode coordinate information. As illustrated in Fig.1c, tokens within \mathcal{X}_t are augmented with identical temporal positional encodings before the first layer, denoting their frame order within the current clip (e.g., \mathcal{X}_{t-T} at position 0, \mathcal{X}_t at position T). Prior to linear

¹ h and w are the height and width of the bbox.

projection to K and V , each token is added with a spatial positional encoding derived from its own coordinates, thereby emphasizing spatial location information.

3.3 Training

Unlike large language model pre-training, where each output token is required to predict the next word in a fixed vocabulary table via classification, in MOT, the same individual object generates a unique trajectory, making it impractical to establish a fixed individual object vocabulary. While MOTIP proposes using a shared tracking ID dictionary to predict the ID labels of current detected objects, determining the appropriate dictionary size requires empirical tuning for different datasets, and there is a risk of ID exhaustion when the number of tracked objects exceeds the dictionary size.

To ensure generalizability, PuTR circumvents the ID dictionary and instead leverages the relative affinity matrix to classify the current detected objects, thus accomplishing the association task. Specifically, we calculate the inner product between \mathcal{Z}_{t-1} and \mathcal{Z}_t , i.e., $\mathcal{Z}_{t-1}\mathcal{Z}_t^\top$ ($t \geq 1$), to obtain the affinity matrix, and apply the softmax along rows to get the probability distribution of the previous objects corresponding to the next objects. Through this, we can determine the association via the Hungarian algorithm, similar to heuristic methods, without the need for a fixed vocabulary table. The classification loss is therefore simply calculated as the cross-entropy loss between the predicted probability and the ground truth label. Without bells and whistles, the training loss of PuTR is straightforwardly calculated as:

$$\mathcal{L} = \frac{\sum_{bs} \sum^T CE(\text{softmax}_r(\mathcal{Z}_{t-1}\mathcal{Z}_t^\top), Y_t)}{bs \times T}, \quad (1)$$

where $CE(\cdot)$ denotes the cross-entropy loss, Y_t is the ground truth label in the t -th frame, and bs is the batch size. $CE(\cdot)$ calculates the cross-entropy loss between the predicted probability and the ground truth label, averaging over the number of objects in \mathcal{Z}_{t-1} . For an identity tid in \mathcal{Z}_t but not in \mathcal{Z}_{t-1} , we assign the nearest output object embedding with the same tid prior to \mathcal{Z}_{t-1} . This strategy adds long distance training samples to overcome object intervals. To prevent anomalies in loss calculation, no row corresponds to an object in \mathcal{Z}_t that initiates its trajectory, and we also remove rows with tid in \mathcal{Z}_{t-1} but not in \mathcal{Z}_t .

3.4 Inference

Different methodologies are not mutually exclusive. Although DETR-based methods are considered end-to-end, some of them still require a runtime manager to schedule tracklet states [59] and occasionally resolve assignment conflicts between tracklets and detections via heuristic rules or the Hungarian algorithm during inference [16]. From this perspective, they can also be near "Heuristic Methods," with the distinction that the similarity matrix is generated by neural networks instead of handcrafted models. Therefore, it is natural that our proposed PuTR, as a separated framework, incorporates a runtime manager and the Hungarian algorithm to deal with similar issues during inference. Notably, we only match once per frame, emphasizing the Transformer’s capability in solving the association problem, instead of using multiple matching strategies like ByteTrack.

3.4.1 Pipeline

In the first frame of a video sequence during inference, detected objects with a confidence score greater than the tracklet threshold τ_{new} are recorded as newborn objects and assigned unique tracking identities. At each subsequent time step t , we first filter the detection results with a detection threshold τ_{det} . These remaining detections \mathcal{O}_t are then concatenated with the object sequence \mathcal{S} from the recent T frames and fed into PuTR to generate an affinity matrix. We then employ the Hungarian algorithm to obtain assignment results and a runtime manager to update the tracklet states. The unmatched object with a detection confidence greater than τ_{new} will be considered a newborn target and given a new identity. Please refer to Appendix A for more details.

3.4.2 Affinity Matrix

PuTR calculates distances between object features of different frames instead of identifying explicit individuals due to the absence of an ID dictionary. This approach, however, inevitably disregards

spatial positioning even after adding spatial positional encodings, leading to erroneous matches between visually similar but spatially distant objects. Moreover, occlusions or illumination changes may cause objects from the previous frame ($t - 1$) to vanish or lose discriminative information. To address these issues, we compute the similarity matrix \mathbf{S} on \mathcal{S}_{out} rather than just the last two frames, and incorporate bboxes to compensate for the lack of spatial information. The matrix \mathbf{S} is calculated as:

$$\mathbf{S} = \text{softmax}_r([\mathcal{Z}_{t-T}, \dots, \mathcal{Z}_{t-1}] \mathcal{Z}_t^\top) \cdot \mathbf{I}^\alpha + \mathbf{I}^\beta, \quad (2)$$

where \mathbf{I}^α and \mathbf{I}^β are IoU matrices to compensate for the similarity in object scale and position, respectively. We compute \mathbf{I}^α between the bboxes of $[\mathcal{O}_{t-T}, \dots, \mathcal{O}_{t-1}]$ and detections \mathcal{O}_t . To focus solely on object scale, we calculate IoU after setting the center coordinates of all bboxes to zero while preserving their width and height. \mathbf{I}^β is the standard IoU between trajectory bboxes² of $[\mathcal{O}_{t-T}, \dots, \mathcal{O}_{t-1}]$ and \mathcal{O}_t to focus on the object position. Please refer to Appendix B for detailed explanations. Each row of \mathbf{S} represents the similarity between an object in previous frames and all objects in the current frame. We then take the maximum value under the same trajectory for each detection to obtain the trajectory-detection affinity matrix \mathbf{A} , where each row represents the similarity between a trajectory and all current detections. The maximum operation ensures the overall similarity is governed by the most distinctive pair, enhancing robustness. Inspired by heuristic methods, we use a weight matrix \mathbf{W} to further prune invalid matches from bipartite matching. \mathbf{W} has the same shape as \mathbf{A} and is calculated as:

$$\mathbf{W}_{ij} = \mathbf{H}_{ij} \cdot \mathbf{T}_i \cdot \mathbf{D}_j \quad (3)$$

where \mathbf{H} is the Height Modulated IoU from Hybrid-SORT [52], calculated using trajectory and detection bboxes; \mathbf{T}_i and \mathbf{D}_j are the confidence scores of the i -th trajectory and j -th detection, following FastTrack [25]. Finally, we employ the Hungarian algorithm on $\mathbf{A} \cdot \mathbf{W}$ to obtain the final assignment results.

4 Experiments

4.1 Settings

4.1.1 Datasets

For comprehensive analysis, we evaluate PuTR on four MOT benchmarks: MOT17, MOT20, DanceTrack, and the recently proposed SportsMOT. These datasets represent diverse tracking scenarios with distinct characteristics. MOT17 and MOT20 focus on pedestrian tracking with relatively regular motion patterns. MOT17 typically contains sparse pedestrians at small scales, while MOT20 features dense crowds (over 100 people per frame) at larger scales. DanceTrack presents challenging scenarios with performers executing complex movements on stage, characterized by frequent directional changes and mutual occlusions. SportsMOT encompasses various athletic scenarios (basketball, football, volleyball), featuring rapid movements and variable object speeds between adjacent frames.

The test sets of MOT17 and MOT20 contain limited sequences (7 and 4, respectively), which has led to practices like per-sequence threshold tuning and post-interpolation in heuristic methods. Such practices may compromise the reliability of performance metrics. In contrast, SportsMOT and DanceTrack provide substantially larger test sets (35 and 150, respectively), making such optimizations impractical and yielding more dependable evaluation results.

4.1.2 Metrics

We employ three widely-used metrics: HOTA [28], IDF1 [35], and MOTA [3]. MOTA measures object coverage, IDF1 focuses on identity preservation, and HOTA strikes a balance between these two aspects. Within HOTA, AssA assesses association performance, while DetA evaluates detection performance. When methods are evaluated on the same detection results, MOTA values are nearly identical across methods. HOTA and IDF1 can better reflect the performance of the association component.

²The bbox/confidence score of a trajectory is from the object with the largest frame index in the same *tid*, following heuristic methods.

Table 1: Ablations on the affinity matrix. The Compensation, **H**, **T**, and **D** indicate the use of the similarity compensation, Height Modulated IoU, trajectory confidence score, and detection confidence score, respectively.

Affinity Matrix				SportsMOT val			DanceTrack val		
Compensation	H	T	D	HOTA \uparrow	MOTA \uparrow	IDF1 \uparrow	HOTA \uparrow	MOTA \uparrow	IDF1 \uparrow
				76.8	95.7	78.7	52.3	88.7	52.8
✓				78.4	95.8	80.7	55.0	88.9	55.5
✓	✓			78.7	95.8	81.0	55.4	89.1	56.0
✓	✓	✓		78.7	95.8	81.1	56.0	89.2	57.4
✓	✓	✓	✓	78.9	95.8	81.2	57.3	89.3	58.7
✓	✓	✓	✓	78.9	95.8	81.2	57.6	89.4	59.4

Table 2: Ablations on the attention mask. Mask denotes the type of mask in the self-attention mechanism, and Shuffle indicates whether the object sequence of the current frame is shuffled during inference.

PuTR		SportsMOT val			DanceTrack val		
Mask	Shuffle	HOTA \uparrow	MOTA \uparrow	IDF1 \uparrow	HOTA \uparrow	MOTA \uparrow	IDF1 \uparrow
causal		77.9	95.6	80.3	55.7	88.8	57.7
causal	✓	77.5	95.7	80.0	55.9	88.8	57.9
frame causal		78.9	95.8	81.2	57.6	89.4	59.4
frame causal	✓	78.9	95.8	81.2	57.6	89.4	59.4

4.1.3 Implementation Details

To enhance the efficiency, we adopt several strategies when establishing PuTR with PyTorch. We leverage the `grid_sample` function³ to simultaneously sample the grid center points of all objects within a frame. Moreover, the `scaled_dot_product_attention` function⁴ is employed to accelerate the calculation of the attention mechanism during both training and inference. Additionally, we implement a runtime manager following FastTrack [25], maintaining active tracklets in a tensor array instead of a list of Python entities, thereby facilitating parallel processing and further improving efficiency.

Both training and inference of PuTR are conducted on an RTX 4090 GPU. During training, consistent settings are maintained across all datasets for simplicity. PuTR is optimized using the AdamW optimizer and a cosine learning rate schedule with a batch size of 4 for 7 epochs on the corresponding training set. The length of training clips is progressively increased from 4 to 8, 16, 32, 64, and 128 at the 2nd, 3rd, 4th, 5th, and 6th epoch, respectively, except on MOT20, where the clip length stays at 64 after the 6th epoch due to GPU memory limitations. The initial learning rate is set to 0.0002. We apply weight decay of 0.0005, gradient clipping of 1.0, and accumulate gradients for 32 steps. Following the practices of previous works [59; 15], training clips are sampled from the training sequences with a random interval ranging from 1 to 10, and augmented with random cropping, random resizing, HSV color jittering, and random horizontal flipping to enhance diversity.

During inference, we adopt publicly available YOLOX detections for a fair comparison. The detection results for DanceTrack are obtained from <https://github.com/DanceTrack/DanceTrack>, for MOT17 and MOT20 from <https://github.com/ifzhang/ByteTrack>, and for SportsMOT from <https://github.com/MCG-NJU/MixSort>. The consecutive frame T is set to 30 for all datasets. Hyperparameters are consistent within the same dataset and not specifically tuned for each test sequence. We maintain consistent hyperparameters within each test set *without per-sequence threshold tuning and post-interpolation*. In the inference stage, we set the confidence threshold τ_{det} to 0.1 across all four datasets. The newborn threshold τ_{new} is set to 0.6 for SportsMOT and DanceTrack, 0.7 for MOT17, and 0.4 for MOT20, generally following the practices of previous works [60; 7].

4.2 Ablation Studies

We conduct comprehensive ablation studies on the SportsMOT and DanceTrack datasets, leveraging their extensive training data and official validation sets.

³`torch.nn.functional.grid_sample`

⁴`torch.nn.functional.scaled_dot_product_attention`

Table 3: Ablations on the positional encoding. Temporal and Spatial denote the use of temporal positional encoding and spatial positional encoding, respectively.

Positional Encoding		SportsMOT val			DanceTrack val		
Temporal	Spatial	HOTA \uparrow	MOTA \uparrow	IDF1 \uparrow	HOTA \uparrow	MOTA \uparrow	IDF1 \uparrow
		78.7	95.8	80.9	57.1	89.3	58.2
✓		78.8	95.8	81.0	57.4	89.4	58.8
✓	✓	78.9	95.8	81.2	57.6	89.4	59.4

Table 4: Ablations on the input frame length. The T denotes the length of the input frame sequence.

PuTR T	SportsMOT val				DanceTrack val			
	HOTA \uparrow	MOTA \uparrow	IDF1 \uparrow	FPS \uparrow	HOTA \uparrow	MOTA \uparrow	IDF1 \uparrow	FPS \uparrow
5	76.6	95.7	77.2	78	56.2	89.4	55.3	77
15	78.0	95.8	79.6	77	57.8	89.6	59.3	76
30	78.9	95.8	81.2	77	57.6	89.4	59.4	75
45	79.1	95.7	81.8	76	58.3	89.3	60.8	74
60	79.1	95.7	82.0	75	56.5	89.2	58.3	73
90	79.0	95.7	82.2	73	56.6	89.0	58.6	71
120	79.4	95.7	83.0	70	56.2	88.8	58.5	68

4.2.1 Affinity Matrix

We analyze the contribution of different components in the affinity matrix, with results presented in Tab.1. In the first row, our baseline implementation of PuTR achieves competitive performance on both validation sets using the maximum operation alone. Experimental results demonstrate that each additional component contributes incrementally to the overall tracking performance. The performance gains are particularly notable on DanceTrack, where improvements exceed those observed on SportsMOT. This differential impact can be attributed to DanceTrack’s higher object density and inter-object similarity, which introduces additional complexity in the feature-based similarity matrix. These characteristics necessitate more sophisticated compensation mechanisms to effectively filter invalid matches during bipartite matching.

4.2.2 Attention Mask

Tab.2 presents our comparative analysis of the proposed frame causal mask against the conventional causal mask. We train and evaluate models using consistent mask types, incorporating random shuffling of current frame object orders during inference. While the association results should theoretically remain invariant to object ordering in the current frame, the conventional causal mask intrinsically couples the training object order with feature extraction, introducing suboptimal constraints for the association task. This coupling manifests in performance degradation, as evidenced by the inconsistent results under shuffled object orders in the first two rows. In contrast, our frame causal mask maintains permutation invariance for objects within the same frame, effectively decoupling object order from association results. The last two rows demonstrate consistent performance across different object orderings, highlighting the stability and reliability of our approach in maintaining consistency between the trajectory graph and Transformer architecture.

4.2.3 Positional Encoding

The effectiveness of our modified positional encodings is quantitatively demonstrated in Tab.3. Experimental results confirm that each encoding component contributes meaningfully to performance improvements across both datasets. The impact is particularly pronounced on DanceTrack, where the high density and visual similarity of dancers necessitate robust temporal and spatial information to effectively distinguish between visually similar objects. This requirement explains the more substantial improvements observed on DanceTrack compared to SportsMOT.

4.2.4 Input Frame Length

We investigate the impact of varying input frame lengths on tracking performance, as shown in Tab.4. Increasing the frame length from 5 to 120 frames consistently improves the association metrics (IDF1 and HOTA) on SportsMOT, reaching peak performance at 120 frames. In contrast, DanceTrack achieves optimal performance at 45 frames.

Table 5: Ablations on the structure parameters. The d_{model} and layers denote the model dimension and the number of layers in PuTR, respectively.

d_{model}	PuTR		SportsMOT val			DanceTrack val		
	layers	HOTA \uparrow	MOTA \uparrow	IDF1 \uparrow	HOTA \uparrow	MOTA \uparrow	IDF1 \uparrow	
256	3	79.0	95.8	81.3	56.5	89.4	57.6	
256	6	78.8	95.8	81.0	57.3	89.5	59.0	
256	9	78.9	95.8	81.3	56.6	89.3	58.2	
512	3	78.9	95.8	81.2	58.3	89.4	60.2	
512	6	78.9	95.8	81.2	57.6	89.4	59.4	
512	9	78.7	95.8	81.0	57.4	89.6	59.0	

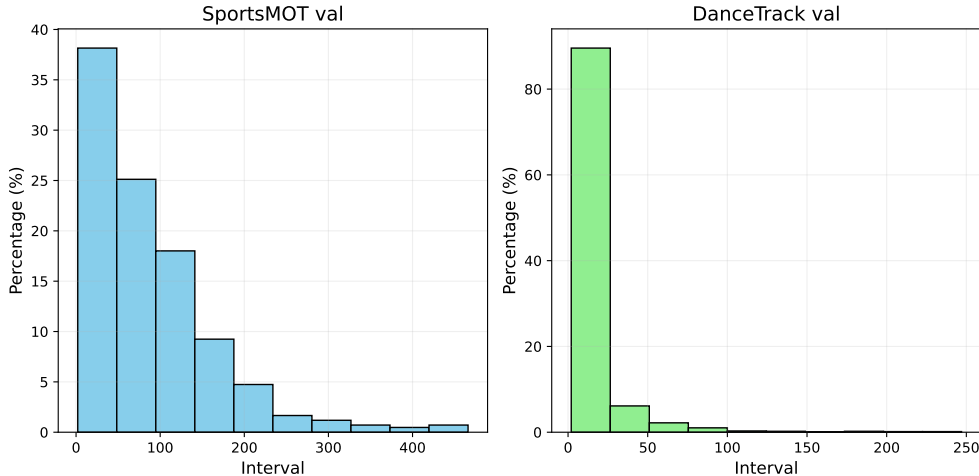


Figure 2: Distribution of object disappearance intervals in the SportsMOT and DanceTrack validation datasets. For each tracked identity, we compute the temporal gap (Interval, the x-axis) between adjacent detections by calculating the difference between current and previous frame numbers, while the y-axis shows their percentage among all non-consecutive cases (interval > 1).

This performance difference stems from distinct camera setups between datasets. SportsMOT employs dynamic cameras that follow competition highlights, causing frequent object entries and exits from the frame. DanceTrack uses fixed cameras capturing the entire stage, where object disappearances mainly result from inter-object occlusions. As illustrated in Fig.2, SportsMOT exhibits significantly longer disappearance intervals (87 frames on average) compared to DanceTrack (12 frames on average), necessitating extended temporal context for identity maintenance.

Notably, Fig.2 only depicts non-consecutive intervals, while consecutive tracking (interval = 1) dominates modern MOT datasets, accounting for over 99% of all cases. This prevalence of short-term connections explains the historical success of heuristic tracking methods. Guided by our intuitive idea, our proposed PuTR naturally unifies both short-term and long-term tracking within a single Transformer architecture while maintaining efficient inference speeds of 70 FPS on SportsMOT and 68 FPS on DanceTrack with 120-frame inputs.

4.2.5 Structure Parameters

We analyze the influence of structure parameters on tracking performance, as shown in Tab.5. Our experiments reveal that performance varies with the number of layers and model dimension. On SportsMOT, optimal performance is achieved with 3 layers and a model dimension of 256, while DanceTrack performs best with 3 layers and a dimension of 512.

However, rather than extensively tuning every hyperparameters for each dataset, we prioritize validating our core methodology through a straightforward implementation of PuTR. *In subsequent experiments, we maintain consistent hyperparameters across datasets as much as possible to demon-*

Table 6: Comparisons with other foundational online methods. The blue background indicates the use of the same detector, where results highlighted in **bold** represents the best results within each column, respectively. PuTR₁₂₀ denotes the model tested with a longer sequence length of 120 frames. The offline interpolation and the per-sequence thresholds in ByteTrack and OC-SORT are removed for fair comparison.

Method	HOTA \uparrow	MOTA \uparrow	IDF1 \uparrow	DetA \uparrow	AssA \uparrow
<i>Detector-based:</i>					
Tracktor++ [2]	-	-	-	-	-
CenterTrack [62]	62.7	90.8	60.0	82.1	48.0
FairMOT [61]	49.3	86.4	53.5	70.2	34.7
QDTrack [32]	60.4	90.1	62.3	77.5	47.2
TrackFormer [30]	-	-	-	-	-
MOTR [58]	-	-	-	-	-
MOTIP [16]	71.9	92.9	75.0	83.4	62.0
<i>Heuristic:</i>					
DeepSORT [48]	-	-	-	-	-
ByteTrack [60]	64.1	95.9	71.4	78.5	52.3
OC-SORT [7]	73.7	96.5	74.0	88.5	61.5
PuTR (Ours)	76.0	97.1	77.1	89.3	64.8
PuTR ₁₂₀ (Ours)	76.8	97.1	79.5	89.2	66.2

(a) SportsMOT test set

Method	HOTA \uparrow	MOTA \uparrow	IDF1 \uparrow	DetA \uparrow	AssA \uparrow
<i>Detector-based:</i>					
Tracktor++ [2]	-	-	-	-	-
CenterTrack [62]	41.8	86.8	35.7	78.1	22.6
FairMOT [61]	39.7	82.2	40.8	66.7	23.8
QDTrack [32]	54.2	87.7	50.4	80.1	36.8
TrackFormer [30]	-	-	-	-	-
MOTR [58]	54.2	79.7	51.5	73.5	40.2
MOTIP [16]	67.5	90.3	72.2	79.4	57.6
<i>Heuristic:</i>					
DeepSORT [48]	45.6	87.8	47.9	71.0	29.7
ByteTrack [60]	47.7	89.6	53.9	71.0	32.1
OC-SORT [7]	55.1	92.0	54.6	80.3	38.3
PuTR (Ours)	60.6	92.3	61.7	82.6	44.6

(b) DanceTrack test set

Method	HOTA \uparrow	MOTA \uparrow	IDF1 \uparrow	DetA \uparrow	AssA \uparrow
<i>Detector-based:</i>					
Tracktor++ [2]	42.1	53.5	52.3	42.9	41.7
CenterTrack [62]	52.2	67.8	64.7	53.8	51.0
FairMOT [61]	59.3	73.7	72.3	60.9	58.0
QDTrack [32]	53.9	68.7	66.3	55.6	52.7
TrackFormer [30]	57.3	74.1	68.0	60.9	54.1
MOTR [58]	57.2	71.9	68.4	58.9	55.8
MOTIP [16]	59.2	75.5	71.2	62.0	56.9
<i>Heuristic:</i>					
DeepSORT [48]	61.2	78.0	74.5	63.1	59.7
ByteTrack [60]	62.8	78.9	77.2	63.8	62.2
OC-SORT [7]	61.7	76.0	76.2	61.6	62.0
PuTR (Ours)	62.1	78.8	75.6	64.0	60.5

(c) MOT17 test set

Method	HOTA \uparrow	MOTA \uparrow	IDF1 \uparrow	DetA \uparrow	AssA \uparrow
<i>Detector-based:</i>					
Tracktor++ [2]	42.1	52.7	52.6	42.3	42.0
CenterTrack [62]	-	-	-	-	-
FairMOT [61]	54.6	61.8	67.3	54.7	54.7
QDTrack [32]	60.0	74.7	73.8	61.4	58.9
TrackFormer [30]	54.7	68.6	65.7	56.7	53.0
MOTR [58]	-	-	-	-	-
MOTIP [16]	-	-	-	-	-
<i>Heuristic:</i>					
DeepSORT [48]	57.1	71.8	69.6	59.0	55.5
ByteTrack [60]	60.4	74.2	74.5	62.0	59.9
OC-SORT [7]	60.5	73.1	74.4	60.5	60.8
PuTR (Ours)	61.4	75.6	74.6	62.7	60.4

(d) MOT20 test set

strate the solid performance of our approach, even though this will prevent PuTR from achieving optimal performance on each dataset.

4.3 Comparison with Foundational Online Methods

Tab.6 presents results comparing PuTR with foundational online methods on four datasets and Tab.7 exhibits PuTR’s domain adaptation ability in the domain shift test.

4.3.1 Comparison with Heuristic Methods

PuTR demonstrates superior performance on DanceTrack, SportsMOT⁵, and MOT20, while maintaining competitive results on MOT17. Unlike heuristic approaches, PuTR employs a streamlined Transformer architecture that extracts object features and handles various associations uniformly, eliminating the need for handcrafted rules to specify different scenarios.

As illustrated in Fig.3, PuTR effectively models long-range dependencies through its Transformer architecture. This capability enables robust tracking even during extended occlusions and significant position changes, without relying on any motion cues. For instance, the dancer with blue arrow in the top row is successfully tracked despite prolonged occlusion and substantial spatial displacement.

⁵For SportsMOT, we use the official detection results following the Train+Val setup. In the Train setup, the results of PuTR are 74.3%/95.2%/75.7%/87.2%/63.4% on HOTA/MOTA/IDF1/DetA/AssA.



Figure 3: Visual results of PuTR on the #dancetrack0011 video sequence of DanceTrack (top row) and the #v_1UDUODIBSc_c004 video sequence of SportsMOT (bottom row), showcasing the model’s capability to handle challenging scenarios such as extended occlusions (the blue arrow), and the individual moving out of and re-entering the camera view (the dark arrow).

Similarly, PuTR maintains tracking continuity when subjects exit and re-enter the camera view, as demonstrated by the athlete with dark arrow in the bottom row.

This approach inherently addresses challenges that typically require explicit handling in heuristic methods, such as non-linear motion [25], low frame rates [27], and camera motion [55]. On DanceTrack, despite complex choreographic interactions, PuTR surpasses the second-best method, OC-SORT, with an IDF1 score of 61.7% versus 54.6%. When extending the consecutive frame window to $T = 120$ on SportsMOT, PuTR₁₂₀ achieves remarkable scores of 76.8%/97.1%/79.5% on HOTA/MOTA/IDF1, highlighting its robust long-term tracking capabilities.

However, PuTR shows limitations in processing small-scale objects especially in the low-resolution images of MOT17, as depicted in Fig.4. The abundance of tiny bboxes in MOT17 poses challenges for feature-based association, while motion models handle such cases more effectively. This limitation explains why PuTR, like other detector-based approaches, falls short of heuristic methods’ performance on MOT17.

4.3.2 Comparison with Detector-based Methods

PuTR outperforms the representative JDE [61; 32], CNN-based [2; 62], and DETR-based [30; 58] methods on all benchmarks, except the latest DETR-based approach MOTIP [16] warranting a detailed analysis.

MOTIP leverages its methodology’s advantages but requires additional training data and substantial computational resources (typically 8 GPUs for days) to achieve satisfactory performance, hence excelling on DanceTrack and SportsMOT. For MOT17, the CrowdHuman [40] dataset, containing massive human images, is incorporated following prior work [58; 15] to mitigate overfitting, improving performance while increasing training complexity. For MOT20, where the average pedestrian count per frame exceeds DETR’s detection capacity, only the early TrackFormer [30] is evaluated by modifying Deformable-DETR, while later incremental works focus on datasets with more moderate object query numbers. In contrast, PuTR performs streamlined training from scratch on a single GPU in 1 hour⁶ without any additional data or pretraining, regardless of dataset scale or object count.

PuTR demonstrates superior performance on SportsMOT compared to MOTIP, while exhibiting potential for improvement on DanceTrack. The performance gap on DanceTrack can be attributed to the inherent complexity of dancer interactions, where the YOLOX detector encounters challenges in generating accurate detections under severe occlusion and crowded scenarios. Analysis of the HOTA metric reveals PuTR’s superior performance compared to other heuristic approaches, indicating robust handling of detection inaccuracies. However, the lower AssA score relative to MOTIP suggests that MOTIP’s end-to-end approach with shared ID dictionary is more effective in maintaining identity consistency and filtering inaccurate detections in extreme interaction scenarios. Nevertheless, MOTIP’s advantages come at the cost of increased training complexity and reduced domain adaptability. These observations underscore a fundamental trade-off in MOT: no single methodology can optimally address all MOT challenges simultaneously. By leveraging precise detections, PuTR maximizes

⁶Specifically, training time on DanceTrack, SportsMOT, MOT17, and MOT20 is 60, 40, 30, and 35 minutes.



Figure 4: An example of the failure case in video sequence #MOT17-14 of MOT17. The tiny pink bbox changes individuals twice in the second and fourth frame, due to the weak appearance cues.

Table 7: Domain shift analysis of PuTR across different datasets. Models trained on individual datasets (indicated by subscripts) are evaluated on all test sets. Δ_{max} denotes the maximum performance gap observed across the four test sets, reflecting the model’s domain adaptation capability.

Method	SportsMOT test			DanceTrack test			MOT17 test			MOT20 test		
	HOTA \uparrow	MOTA \uparrow	IDF1 \uparrow	HOTA \uparrow	MOTA \uparrow	IDF1 \uparrow	HOTA \uparrow	MOTA \uparrow	IDF1 \uparrow	HOTA \uparrow	MOTA \uparrow	IDF1 \uparrow
PuTR _{MOT17}	75.7	97.0	76.4	59.5	92.2	60.2	62.1	78.8	75.6	61.3	75.6	74.5
PuTR _{MOT20}	75.9	97.1	77.0	58.9	92.2	59.4	62.1	78.8	75.6	61.4	75.6	74.6
PuTR _{DanceTrack}	75.9	97.1	76.6	60.6	92.3	61.7	61.9	78.9	75.3	61.1	75.4	74.2
PuTR _{SportsMOT}	76.0	97.1	77.1	59.4	92.2	60.2	61.9	79.0	75.5	61.4	75.6	74.8
Δ_{max}	0.3	0.1	0.7	1.7	0.1	2.3	0.2	0.2	0.3	0.3	0.2	0.6

its association capabilities, achieving state-of-the-art results on SportsMOT. Notably, even with additional image data, MOTIP fails to surpass PuTR’s performance on MOT17. Furthermore, PuTR demonstrates strong scalability, extending effectively to dense scenarios in MOT20.

In the inference efficiency, PuTR demonstrates remarkable inference speed. Unlike MOTIP’s 22 FPS⁷ on DanceTrack, SportsMOT, and MOT17, PuTR can process video sequences at a much higher frame rate due to its relatively simple architecture. Specifically, PuTR’s average FPS on the sparse DanceTrack, SportsMOT, and MOT17 datasets are 75, 77, and 62, respectively. Even on the dense MOT20 dataset, it can still achieve an impressive 25 FPS. While the massive number of tracked objects per frame in MOT20 can lengthen the input object sequence and consequently slow down the speed, it still meets real-time requirements. Moreover, the separated approach offers the advantage of independent execution for detection and association, enabling parallel processing pipelines for further efficiency enhancement.

4.3.3 Domain Adaptation Ability

Robust association ability across various scenarios is crucial for MOT methods. Heuristic methods can tune hyperparameters to adapt to most common cases, while other learning-based methods rarely report their domain adaptation ability across datasets despite the urge to address this issue. Only the work [39] specifically addresses the domain adaptation problem in MOT, reporting that QDTrack exhibits a striking degradation, decreasing by 49% in IDF1 and 35% in HOTA when evaluated on DanceTrack with weights trained on MOT17. We also evaluate the official MOTIP weights trained on MOT17 on the DanceTrack test set, only yielding 44.9% IDF1 and 43.0% HOTA.

In contrast, from the domain shift analysis in Tab.7, we find that PuTR has excellent domain adaptation ability across domains. Without any other operation, just applying the weights trained on one dataset to another, the maximum cross-dataset gap is only 2.3% in IDF1 and 1.7% in HOTA, which has never been reported in previous learning-based works. This property of PuTR can be attributed to the fact that it takes advantage of different methodologies, which is appropriate in terms of methodological cross-pollination and integration. It is the separated manner that PuTR can obtain precise detection results like heuristic methods, and the self-attention mechanism of the Transformer that can discriminate individuals in the feature space, even in scenes that have never been trained. Furthermore, the affinity matrix also plays a crucial role, as it circumvents concerns regarding the dictionary capacity or the exhaustion issue in MOTIP. This property makes the new direction we

⁷We test the official model’s speed on the same machine as PuTR and exceed the original 16 FPS report.

proposed more fascinating, and we believe it will attract more attention in the future and promote a new development in the MOT field.

5 Discussion

Through above extensive experiments and analyzes, we have demonstrated PuTR’s effectiveness across diverse tracking scenarios. While there remains a performance gap between PuTR and state-of-the-art incremental methods, our primary contribution lies in establishing the viability of a pure Transformer architecture for modeling the association problem in MOT. The experimental results validate this architectural direction and reveal the potential of Transformer-based approaches for tackling MOT association challenges. Besides the ground-based scenarios, PuTR may also be applicable to UAV tracking tasks [19; 49; 53], as the capability to track objects from fast-moving cameras shown in the SportsMOT dataset suggests.

Furthermore, we outline potential future directions for exploration:

- **Model Capacity.** The results in Tab.5 show that simply increasing the model size does not consistently improve PuTR’s performance. Despite using the same decoder-only architecture as Large Language Models (LLMs), effective scaling of PuTR requires further investigation to achieve the impressive perceptual capabilities of modern LLMs.
- **Motion Cues.** Our current method solely employs the coordinate information of objects. However, as illustrated in Fig.4, PuTR struggles with false matches between small objects in the MOT17 dataset due to insufficient appearance cues for re-identification. Incorporating motion cues, such as displacement and velocity, could alleviate this issue by providing additional discriminative information, especially in challenging scenarios involving tiny objects.

In summary, this work pioneers an innovative Transformer-based direction for MOT. The self-attention-driven modeling of trajectories showcased in PuTR opens up exciting possibilities for further advancements in this crucial computer vision task.

6 Conclusion

In this work, we introduce a novel idea to MOT by demonstrating that trajectory graphs can be effectively modeled using a classical Transformer architecture in a separated and online manner. This idea successfully unifies short- and long-term tracking within a single framework. We validate this concept through our proposed Pure Transformer (PuTR) architecture, which achieves competitive performance while maintaining computational efficiency. Extensive experimental results across multiple datasets demonstrate that PuTR not only achieves solid tracking performance but also exhibits robust domain adaptation capabilities. Our findings establish a promising foundation for future MOT research.

References

- [1] Nir Aharon, Roy Orfaig, and Ben-Zion Bobrovsky. Bot-sort: Robust associations multi-pedestrian tracking. [arXiv preprint arXiv:2206.14651](#), 2022.
- [2] Philipp Bergmann, Tim Meinhardt, and Laura Leal-Taixe. Tracking without bells and whistles. In [Proceedings of the IEEE/CVF international conference on computer vision](#), pages 941–951, 2019.
- [3] Keni Bernardin and Rainer Stiefelagen. Evaluating multiple object tracking performance: the clear mot metrics. [EURASIP Journal on Image and Video Processing](#), 2008:1–10, 2008.
- [4] Alex Bewley, Zongyuan Ge, Lionel Ott, Fabio Ramos, and Ben Upcroft. Simple online and realtime tracking. In [2016 IEEE international conference on image processing \(ICIP\)](#), pages 3464–3468. IEEE, 2016.
- [5] Guillem Brasó and Laura Leal-Taixé. Learning a neural solver for multiple object tracking. In [Proceedings of the IEEE/CVF conference on computer vision and pattern recognition](#), pages 6247–6257, 2020.

- [6] Jiarui Cai, Mingze Xu, Wei Li, Yuanjun Xiong, Wei Xia, Zhuowen Tu, and Stefano Soatto. Memot: Multi-object tracking with memory. In Proceedings of the IEEE/CVF Conference on Computer Vision and Pattern Recognition, pages 8090–8100, 2022.
- [7] Jinkun Cao, Jiangmiao Pang, Xinshuo Weng, Rawal Khirodkar, and Kris Kitani. Observation-centric sort: Rethinking sort for robust multi-object tracking. In Proceedings of the IEEE/CVF conference on computer vision and pattern recognition, pages 9686–9696, 2023.
- [8] Nicolas Carion, Francisco Massa, Gabriel Synnaeve, Nicolas Usunier, Alexander Kirillov, and Sergey Zagoruyko. End-to-end object detection with transformers. In European conference on computer vision, pages 213–229. Springer, 2020.
- [9] Orcun Cetintas, Guillem Brasó, and Laura Leal-Taixé. Unifying short and long-term tracking with graph hierarchies. In Proceedings of the IEEE/CVF Conference on Computer Vision and Pattern Recognition, pages 22877–22887, 2023.
- [10] Yutao Cui, Chenkai Zeng, Xiaoyu Zhao, Yichun Yang, Gangshan Wu, and Limin Wang. Sportsmot: A large multi-object tracking dataset in multiple sports scenes. In Proceedings of the IEEE/CVF International Conference on Computer Vision, pages 9921–9931, 2023.
- [11] Patrick Dendorfer, Hamid Rezatofighi, Anton Milan, Javen Shi, Daniel Cremers, Ian Reid, Stefan Roth, Konrad Schindler, and Laura Leal-Taixé. Mot20: A benchmark for multi object tracking in crowded scenes. arXiv preprint arXiv:2003.09003, 2020.
- [12] Yunhao Du, Zhicheng Zhao, Yang Song, Yanyun Zhao, Fei Su, Tao Gong, and Hongying Meng. Strongsort: Make deepsort great again. IEEE Transactions on Multimedia, 2023.
- [13] Mohamed Elhoseny. Multi-object detection and tracking (modt) machine learning model for real-time video surveillance systems. Circuits, Systems, and Signal Processing, 39(2):611–630, 2020.
- [14] Andreas Ess, Konrad Schindler, Bastian Leibe, and Luc Van Gool. Object detection and tracking for autonomous navigation in dynamic environments. The International Journal of Robotics Research, 29(14):1707–1725, 2010.
- [15] Ruopeng Gao and Limin Wang. Memotr: Long-term memory-augmented transformer for multi-object tracking. In Proceedings of the IEEE/CVF International Conference on Computer Vision, pages 9901–9910, 2023.
- [16] Ruopeng Gao, Yijun Zhang, and Limin Wang. Multiple object tracking as id prediction. arXiv preprint arXiv:2403.16848, 2024.
- [17] Zheng Ge, Songtao Liu, Feng Wang, Zeming Li, and Jian Sun. Yolox: Exceeding yolo series in 2021. arXiv preprint arXiv:2107.08430, 2021.
- [18] Wen Guo, Wuzhou Quan, Junyu Gao, Tianzhu Zhang, and Changsheng Xu. Feature disentanglement network: Multi-object tracking needs more differentiated features. ACM Transactions on Multimedia Computing, Communications and Applications, 20(3):1–22, 2023.
- [19] Bing He, Fasheng Wang, Xing Wang, Haojie Li, Fuming Sun, and Hui Zhou. Temporal context and environment-aware correlation filter for uav object tracking. IEEE Transactions on Geoscience and Remote Sensing, 2024.
- [20] Weiming Hu, Tieniu Tan, Liang Wang, and Steve Maybank. A survey on visual surveillance of object motion and behaviors. IEEE Transactions on Systems, Man, and Cybernetics, Part C (Applications and Reviews), 34(3):334–352, 2004.
- [21] Cheng Huang, Shoudong Han, Mengyu He, Wenbo Zheng, and Yuhao Wei. Deconfusetrack: Dealing with confusion for multi-object tracking. In Proceedings of the IEEE/CVF Conference on Computer Vision and Pattern Recognition, pages 19290–19299, 2024.
- [22] Hao Jiang, Sidney Fels, and James J Little. A linear programming approach for multiple object tracking. In 2007 IEEE Conference on Computer Vision and Pattern Recognition, pages 1–8. IEEE, 2007.
- [23] R. E. Kalman. A New Approach to Linear Filtering and Prediction Problems. Journal of Basic Engineering, 82(1):35–45, 03 1960.
- [24] Harold W Kuhn. The hungarian method for the assignment problem. Naval research logistics quarterly, 2(1-2):83–97, 1955.

- [25] Chongwei Liu, Haojie Li, and Zhihui Wang. Fasttrack: A highly efficient and generic gpu-based multi-object tracking method with parallel kalman filter. International Journal of Computer Vision, pages 1–21, 2023.
- [26] Shilong Liu, Feng Li, Hao Zhang, Xiao Yang, Xianbiao Qi, Hang Su, Jun Zhu, and Lei Zhang. DAB-DETR: Dynamic anchor boxes are better queries for DETR. In International Conference on Learning Representations, 2022.
- [27] Y. Liu, J. Wu, and Y. Fu. Collaborative tracking learning for frame-rate-insensitive multi-object tracking. In 2023 IEEE/CVF International Conference on Computer Vision (ICCV), pages 9930–9939, Los Alamitos, CA, USA, oct 2023. IEEE Computer Society.
- [28] Jonathon Luiten, Aljosa Osep, Patrick Dendorfer, Philip Torr, Andreas Geiger, Laura Leal-Taixé, and Bastian Leibe. Hota: A higher order metric for evaluating multi-object tracking. International journal of computer vision, 129:548–578, 2021.
- [29] Gerard Maggolino, Adnan Ahmad, Jinkun Cao, and Kris Kitani. Deep oc-sort: Multi-pedestrian tracking by adaptive re-identification. In 2023 IEEE International Conference on Image Processing (ICIP), pages 3025–3029. IEEE, 2023.
- [30] Tim Meinhardt, Alexander Kirillov, Laura Leal-Taixe, and Christoph Feichtenhofer. Trackformer: Multi-object tracking with transformers. In Proceedings of the IEEE/CVF conference on computer vision and pattern recognition, pages 8844–8854, 2022.
- [31] Anton Milan, Laura Leal-Taixé, Ian Reid, Stefan Roth, and Konrad Schindler. Mot16: A benchmark for multi-object tracking. arXiv preprint arXiv:1603.00831, 2016.
- [32] Jiangmiao Pang, Linlu Qiu, Xia Li, Haofeng Chen, Qi Li, Trevor Darrell, and Fisher Yu. Quasi-dense similarity learning for multiple object tracking. In Proceedings of the IEEE/CVF conference on computer vision and pattern recognition, pages 164–173, 2021.
- [33] Hamed Pirsiavash, Deva Ramanan, and Charless C. Fowlkes. Globally-optimal greedy algorithms for tracking a variable number of objects. In CVPR 2011, pages 1201–1208, 2011.
- [34] Shaoqing Ren, Kaiming He, Ross Girshick, and Jian Sun. Faster r-cnn: Towards real-time object detection with region proposal networks. Advances in neural information processing systems, 28, 2015.
- [35] Ergys Ristani, Francesco Solera, Roger Zou, Rita Cucchiara, and Carlo Tomasi. Performance measures and a data set for multi-target, multi-camera tracking. In European conference on computer vision, pages 17–35. Springer, 2016.
- [36] Amir Roshan Zamir, Afshin Dehghan, and Mubarak Shah. Gmcp-tracker: Global multi-object tracking using generalized minimum clique graphs. In Computer Vision–ECCV 2012: 12th European Conference on Computer Vision, Florence, Italy, October 7–13, 2012, Proceedings, Part II 12, pages 343–356. Springer, 2012.
- [37] David E Rumelhart, Geoffrey E Hinton, and Ronald J Williams. Learning representations by back-propagating errors. nature, 323(6088):533–536, 1986.
- [38] Franco Scarselli, Marco Gori, Ah Chung Tsoi, Markus Hagenbuchner, and Gabriele Monfardini. The graph neural network model. IEEE transactions on neural networks, 20(1):61–80, 2008.
- [39] Mattia Segu, Bernt Schiele, and Fisher Yu. DARTH: Holistic test-time adaptation for multiple object tracking. In Proceedings of the IEEE/CVF International Conference on Computer Vision, pages 9717–9727, 2023.
- [40] Shuai Shao, Zijian Zhao, Boxun Li, Tete Xiao, Gang Yu, Xiangyu Zhang, and Jian Sun. Crowdhuman: A benchmark for detecting human in a crowd. arXiv preprint arXiv:1805.00123, 2018.
- [41] Peize Sun, Jinkun Cao, Yi Jiang, Zehuan Yuan, Song Bai, Kris Kitani, and Ping Luo. Dancetrack: Multi-object tracking in uniform appearance and diverse motion. In Proceedings of the IEEE/CVF Conference on Computer Vision and Pattern Recognition, pages 20993–21002, 2022.
- [42] ShiJie Sun, Naveed Akhtar, HuanSheng Song, Ajmal Mian, and Mubarak Shah. Deep affinity network for multiple object tracking. IEEE transactions on pattern analysis and machine intelligence, 43(1):104–119, 2019.
- [43] Siyu Tang, Mykhaylo Andriluka, Bjoern Andres, and Bernt Schiele. Multiple people tracking by lifted multicut and person re-identification. In Proceedings of the IEEE conference on computer vision and pattern recognition, pages 3539–3548, 2017.

- [44] Hugo Touvron, Louis Martin, Kevin Stone, Peter Albert, Amjad Almahairi, Yasmine Babaei, Nikolay Bashlykov, Soumya Batra, Prajjwal Bhargava, Shruti Bhosale, et al. Llama 2: Open foundation and fine-tuned chat models. *arXiv preprint arXiv:2307.09288*, 2023.
- [45] Ashish Vaswani, Noam Shazeer, Niki Parmar, Jakob Uszkoreit, Llion Jones, Aidan N Gomez, Łukasz Kaiser, and Illia Polosukhin. Attention is all you need. *Advances in neural information processing systems*, 30, 2017.
- [46] Haidong Wang, Xuan He, Zhiyong Li, Jin Yuan, and Shutao Li. Jdan: Joint detection and association network for real-time online multi-object tracking. *ACM Transactions on Multimedia Computing, Communications and Applications*, 19(1s):1–17, 2023.
- [47] Zhongdao Wang, Liang Zheng, Yixuan Liu, Yali Li, and Shengjin Wang. Towards real-time multi-object tracking. In *European conference on computer vision*, pages 107–122. Springer, 2020.
- [48] Nicolai Wojke, Alex Bewley, and Dietrich Paulus. Simple online and realtime tracking with a deep association metric. In *2017 IEEE international conference on image processing (ICIP)*, pages 3645–3649. IEEE, 2017.
- [49] Qi Xu, Zhuoming Xu, Huabin Wang, Yun Chen, and Liang Tao. Online learning discriminative sparse convolution networks for robust uav object tracking. *Knowledge-Based Systems*, 308:112742, 2025.
- [50] Yihong Xu, Aljosa Osep, Yutong Ban, Radu Horaud, Laura Leal-Taixé, and Xavier Alameda-Pineda. How to train your deep multi-object tracker. In *Proceedings of the IEEE/CVF Conference on Computer Vision and Pattern Recognition*, pages 6787–6796, 2020.
- [51] Feng Yan, Weixin Luo, Yujie Zhong, Yiyang Gan, and Lin Ma. Bridging the gap between end-to-end and non-end-to-end multi-object tracking. *arXiv preprint arXiv:2305.12724*, 2023.
- [52] Mingzhan Yang, Guangxin Han, Bin Yan, Wenhua Zhang, Jinqing Qi, Huchuan Lu, and Dong Wang. Hybrid-sort: Weak cues matter for online multi-object tracking. In *Proceedings of the AAAI Conference on Artificial Intelligence*, volume 38, pages 6504–6512, 2024.
- [53] Mufeng Yao, Jiaqi Wang, Jinlong Peng, Mingmin Chi, and Chao Liu. Folt: Fast multiple object tracking from uav-captured videos based on optical flow. In *Proceedings of the 31st ACM International Conference on Multimedia*, pages 3375–3383, 2023.
- [54] Kefu Yi, Kai Luo, Xiaolei Luo, Jianguai Huang, Hao Wu, Rongdong Hu, and Wei Hao. Ucmctrack: Multi-object tracking with uniform camera motion compensation. In *Proceedings of the AAAI conference on artificial intelligence*, volume 38, pages 6702–6710, 2024.
- [55] Kefu Yi, Kai Luo, Xiaolei Luo, Jianguai Huang, Hao Wu, Rongdong Hu, and Wei Hao. Ucmctrack: Multi-object tracking with uniform camera motion compensation. In *Proceedings of the AAAI Conference on Artificial Intelligence*, volume 38, pages 6702–6710, 2024.
- [56] Sisi You, Hantao Yao, Bing-Kun Bao, and Changsheng Xu. Multi-object tracking with spatial-temporal tracklet association. *ACM Transactions on Multimedia Computing, Communications and Applications*, 20(5):1–21, 2024.
- [57] En Yu, Tiancai Wang, Zhuoling Li, Yuang Zhang, Xiangyu Zhang, and Wenbing Tao. Motrv3: Release-fetch supervision for end-to-end multi-object tracking. *arXiv preprint arXiv:2305.14298*, 2023.
- [58] Fangao Zeng, Bin Dong, Yuang Zhang, Tiancai Wang, Xiangyu Zhang, and Yichen Wei. Motr: End-to-end multiple-object tracking with transformer. In *European Conference on Computer Vision*, pages 659–675. Springer, 2022.
- [59] Y. Zhang, T. Wang, and X. Zhang. Motrv2: Bootstrapping end-to-end multi-object tracking by pretrained object detectors. In *2023 IEEE/CVF Conference on Computer Vision and Pattern Recognition (CVPR)*, pages 22056–22065, Los Alamitos, CA, USA, jun 2023. IEEE Computer Society.
- [60] Yifu Zhang, Peize Sun, Yi Jiang, Dongdong Yu, Fucheng Weng, Zehuan Yuan, Ping Luo, Wenyu Liu, and Xinggang Wang. Bytetrack: Multi-object tracking by associating every detection box. In *European conference on computer vision*, pages 1–21. Springer, 2022.
- [61] Yifu Zhang, Chunyu Wang, Xinggang Wang, Wenjun Zeng, and Wenyu Liu. Fairmot: On the fairness of detection and re-identification in multiple object tracking. *International Journal of Computer Vision*, 129:3069–3087, 2021.

- [62] Xingyi Zhou, Vladlen Koltun, and Philipp Krähenbühl. Tracking objects as points. In European conference on computer vision, pages 474–490. Springer, 2020.
- [63] Xingyi Zhou, Dequan Wang, and Philipp Krähenbühl. Objects as points. arXiv preprint arXiv:1904.07850, 2019.
- [64] Xizhou Zhu, Weijie Su, Lewei Lu, Bin Li, Xiaogang Wang, and Jifeng Dai. Deformable DETR: Deformable transformers for end-to-end object detection. In International Conference on Learning Representations, 2021.

Appendix

A Inference Pipeline

Algorithm 1 Inference pipeline.

Require: A video sequence \mathcal{V} ; a detector $Det(\cdot)$; a lost tolerance T .

- 1: The set of trajectories $\mathcal{T}^* \leftarrow \emptyset$; The set of active trajectories $\mathcal{T}_{active}^* \leftarrow \emptyset$.
- 2: **for** $frame_t$ **in** \mathcal{V} **do**
- /* generate detected objects */
- 3: $\mathcal{O}_t \leftarrow Det(frame_t)$;
- /* generate an affinity matrix */
- 4: $\mathbf{A} \cdot \mathbf{W} \leftarrow GenAffinity(\mathcal{T}_{active}^*, \mathcal{O}_t)$;
- /* associate */
- 5: $\mathcal{O}_m, \mathcal{T}_m^*, \mathcal{O}_u, \mathcal{T}_u^* \leftarrow Hungarian(\mathbf{A} \cdot \mathbf{W})$
- 6: \mathcal{O}_m : matched detections from \mathcal{O}_t ;
- 7: \mathcal{T}_m^* : matched tracklets from \mathcal{T}_{active}^* ;
- 8: \mathcal{O}_u : unmatched detections from \mathcal{O}_t ;
- 9: \mathcal{T}_u^* : unmatched tracklets from \mathcal{T}_{active}^* ;
- /* update tracklets */
- 10: **for** $\mathcal{T}_{tid}, \mathcal{O}_{tid}^t$ **in** $\mathcal{T}_m^*, \mathcal{O}_m$ **do**
- $\mathcal{T}_{tid} \leftarrow Update(\mathcal{T}_{tid}, \mathcal{O}_{tid}^t)$;
- 12: **end for**
- /* remove tracklets */
- 13: **for** \mathcal{T}_{tid} **in** \mathcal{T}_u^* **do**
- if** $LostGap(\mathcal{T}_{tid}) > T$ **or** $\mathcal{T}_{tid}.State == New$ **then**
- $\mathcal{T}_u^* \leftarrow \mathcal{T}_u^* \setminus \{\mathcal{T}_{tid}\}$;
- $\mathcal{T}^* \leftarrow \mathcal{T}^* \cup \{\mathcal{T}_{tid}\}$;
- 17: **else**
- $\mathcal{T}_{tid}.State \leftarrow Lost$;
- 19: **end if**
- 20: **end for**
- 21: $\mathcal{T}_{active}^* \leftarrow \mathcal{T}_m^* \cup \mathcal{T}_u^*$;
- /* initialize new tracklets */
- 22: $\mathcal{T}_{active}^* \leftarrow \mathcal{T}_{active}^* \cup Init(\mathcal{O}_u)$;
- 23: **end for**
- 24: $\mathcal{T}^* \leftarrow \mathcal{T}^* \cup \mathcal{T}_{active}^*$;

Ensure: \mathcal{T}^* .

Algo.1 shows the inference pipeline of our method. The pipeline follows a simple style to SORT, requiring only one association during one frame to highlight the Transformer’s capability in solving the association problem.

The inputs of the pipeline are a video sequence \mathcal{V} , a detector $Det(\cdot)$, and a lost tolerance T (same as the input frame length of PuTR). The output is the set of trajectories \mathcal{T}^* , and we also maintain a set of active trajectories \mathcal{T}_{active}^* to record the tracklets that are not terminated yet. Each tracklet in \mathcal{T}_{active}^* has a state attribute, called *State* (one of *Track*, *Lost*, or *New*), to indicate its status at the current frame.

For each frame $frame_t$ in \mathcal{V} , we obtain the set of detected objects \mathcal{O}_t via $Det(\cdot)$ (line 3), filtering by detection threshold τ_{det} and initializing tracking identities tid to -1 . We then generate an affinity matrix using \mathcal{T}_{active}^* and \mathcal{O}_t through PuTR as described in the main paper (line 4). The Hungarian algorithm then processes $\mathbf{A} \cdot \mathbf{W}$ to obtain the assignment results, i.e., matched objects \mathcal{O}_m , matched tracklets \mathcal{T}_m^* , unmatched detections \mathcal{O}_u , and unmatched tracklets \mathcal{T}_u^* (lines 5 to 9). The objects in \mathcal{O}_m will be updated into the corresponding tracklets in \mathcal{T}_m^* (lines 10 to 12), where the *State* of tracklets will be set to *Track*. Then, the tracklets in \mathcal{T}_u^* will be moved from \mathcal{T}_{active}^* into \mathcal{T}^* if the lost gap is larger than T or its *State* is *New*, following ByteTrack. Otherwise, they will remain in \mathcal{T}_{active}^* , and their *State* will be set to *Lost* (lines 13 to 20). Next, objects in \mathcal{O}_u will be initialized as new tracklets and added into \mathcal{T}_{active}^* after filtering with the tracklet threshold τ_{new} (line 22). Finally, after processing all frames in \mathcal{V} , \mathcal{T}_{active}^* will be merged into \mathcal{T}^* , and \mathcal{T}^* is the final tracking result of the video sequence \mathcal{V} (line 24).

B Similarity Compensation

We elaborate on the IoU matrices \mathbf{I}^α and \mathbf{I}^β used for similarity compensation in the similarity matrix \mathbf{S} .

The design of \mathbf{I}^α and \mathbf{I}^β for similarity matrix compensation is based on a key assumption in heuristic methods: objects belonging to the same individual should exhibit high similarity in both appearance and motion cues across adjacent frames. This implies that for the same individual, high similarity must be present simultaneously in both feature space and bbox scale space, while bbox positions may vary due to rapid movement.

For scale compensation, we utilize only the bbox scale in \mathbf{I}^α to compensate for the feature similarity in the scale space:

$$\mathbf{I}_{ij}^\alpha = \text{IoU}'(\text{bbox}_i, \text{bbox}_j), \tag{4}$$

where bbox_i and bbox_j are the bboxes of the i -th object in $[\mathcal{O}_{t-T}, \dots, \mathcal{O}_{t-1}]$ and the j -th object in \mathcal{O}_t , respectively. A bbox is defined as $[u, v, w, h]$, where u and v are the center coordinates, and w and h are the width and height. $\text{IoU}'(\cdot)$ denotes the IoU score calculated after setting the center coordinates of both bboxes to zero while preserving their width and height. This alignment ensures that the IoU score is not affected by the bbox positions, focusing solely on the object scale. By multiplying \mathbf{I}^α in \mathbf{S} , we emphasize the feature similarity of objects with similar scales.

For position compensation, we leverage the fact that objects appear in close proximity in consecutive frames. We compute the standard IoU score (\mathbf{I}^β) using detections and the last positions of trajectories, following heuristic methods but without introducing any motion model. When computing \mathbf{I}_{ij}^β , bbox_i represents the bbox of the trajectory of the i -th object in $[\mathcal{O}_{t-T}, \dots, \mathcal{O}_{t-1}]$, while bbox_j remains the bbox of the j -th object in \mathcal{O}_t . The trajectory bbox is taken from the object with the largest frame index in the same *tid*, denoting the last position of the trajectory. Since IoU evaluates to zero for disjoint bboxes — a common occurrence for fast-moving objects — we opt to add rather than multiply \mathbf{I}^β in \mathbf{S} . This choice prevents the feature similarity from being completely suppressed by zero IoU scores, ensuring that the model can still identify objects with similar features but different positions. This approach effectively compensates for the feature similarity in the position space.

Through these compensation strategies, we aim to enhance the feature similarity in both scale and position spaces, enabling the model to better distinguish between objects with similar features but different scales or positions.